Journal of Economic Entomology, 2025, **00**, 1–9
DOI: https://doi.org/10.1093/jee/toaf301
Research

Molecular Entomology

Effect of sugar transporter 1 on reproduction of *Nilaparvata lugens* (Hemiptera: Delphacidae) and trehalose metabolism

Yongkang Liu[†,1,2], Yanlin Luo[†,1], Liwen Guan[1], Sijing Wan[1], Xianzhong Wang[1], Caidi Xu[1], Binghua Xie[1], Shigui Wang[1], and Bin Tang[*,1]

[1]College of Life and Environmental Sciences, Hangzhou Normal University, Hangzhou, China
[2]College of Agriculture & Biotechnology, Zhejiang University, Hangzhou, China

[*]Corresponding author. College of Life and Environmental Sciences, Hangzhou Normal University, 2318 Yuhangtang Road, Yuhang District, Hangzhou 311121, China (Email: tbzm611@hznu.edu.cn).

[†]These authors contributed equally to this work.

Subject Editor: Dr. Raul Medina

Sugar transporters play a crucial role in insect life activities, especially in energy metabolism and carbohydrate management. Sugar transporter 1 (*St1*) is a facilitative glucose transporter highly expressed in the midgut of *Nilaparvata lugens* (Stål) (Hemiptera: Delphacidae), however its physiological function remains unclear. To explore its pest control potential, we used RNA interference (RNAi) to investigate *St1*'s effects on sugar metabolism and female reproduction. Silencing *St1* lowered membrane-bound trehalase (TRE2) activity and inhibited the hydrolysis of trehalose into glucose, impeding glycogen accumulation and glucose availability. Our findings show *St1* regulates female reproduction by modulating trehalase activity. This study reveals *St1*'s crucial role in insect physiology and highlights it as a potential target for new, eco-friendly insecticides.

Keywords: sugar transporter, RNAi, trehalose metabolism, reproduction, pest control

Graphical abstract

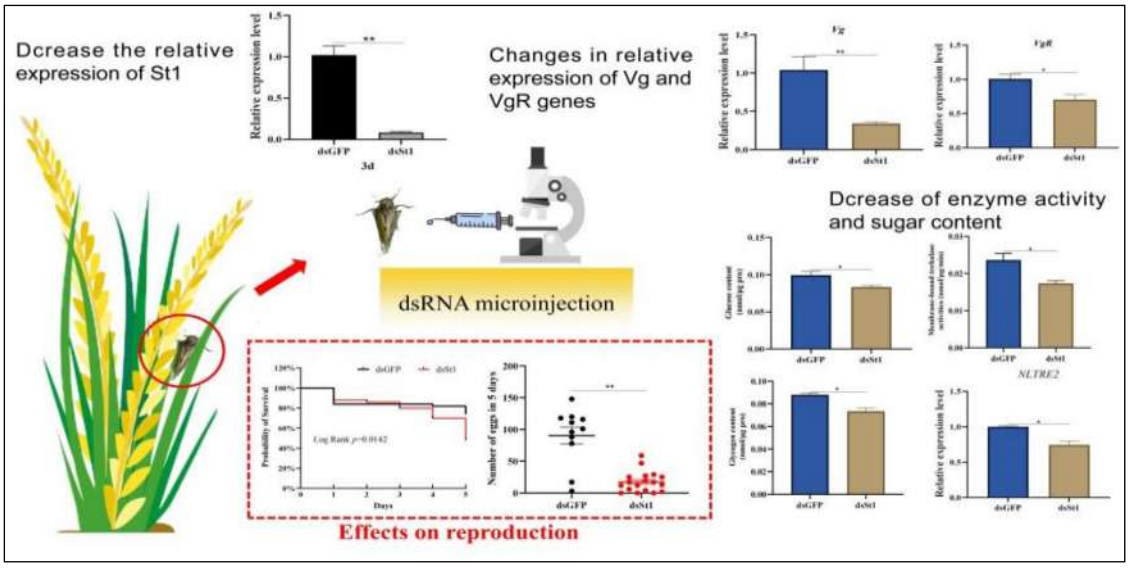

Received: 29 May 2025. **Revised:** 5 October 2025. **Accepted:** 20 October 2025

Introduction

Nilaparvata lugens (Stål) (Hemiptera: Delphacidae), widely distributed in rice-growing regions of eastern, southern, and southeastern Asia, the South Pacific islands, and Australia (Zheng et al. 2021), is a notorious and major migratory pest in Asian rice fields, causing significant crop losses (Ge et al. 2015). Given the widespread insecticide resistance developed by *N. lugens* populations (Yang et al. 2020, Tang et al. 2022, Wang et al. 2022) and its resistance to 33 insecticide active ingredients (Qin et al. 2021), it is urgent to develop new and effective means to control *N. lugens* populations.

Soluble sugars are critical for carbon skeleton formation, energy storage, osmotic regulation, and signaling in organisms. However, since not all tissues and cells can synthesize sugars autonomously, sugar transport emerges as a vital physiological mechanism in living organisms, crucial for maintaining metabolic homeostasis (Chen et al. 2015). Eighteen sugar transporter genes were identified in *N. lugens* (Kikuta et al. 2010). *NlHT1* is a facilitative glucose transporter specifically expressed in the midgut, which was previously identified in *N. lugens* (Price et al. 2007). Sugar transporters, given their crucial roles in metabolic regulation, represent promising candidates as targets for pest control strategies (Ge et al. 2015).

Trehalose, a non-reducing disaccharide, maintains high levels in the hemolymph and is essential as an instant energy source and stress responder in insects (Shukla et al. 2015, Gokulanathan et al. 2024). Trehalose-6-phosphate synthase (*TPS*) catalyzes the synthesis of trehalose from glucose-6-phosphate and UDP-glucose (Shukla et al. 2015, Yang et al. 2017). Trehalose is hydrolyzed into glucose by trehalase (α-glucoside-1-glucohydrolase, *TRE*), an enzyme present in almost all tissues in different forms (Avonce et al. 2006). Previous studies have demonstrated that interfering with *TRE* can disrupt chitin metabolism, resulting in stunted growth and delayed development in *N. lugens* larvae, as well as difficulties in molting and eclosion (Zhao et al. 2016, Tang et al. 2017). Critically, energy metabolism, particularly in relation to trehalose dynamics, serves as the fundamental source of both the substrate and ATP that are indispensable for the biosynthetic processes underlying reproduction.

Vitellogenin (*Vg*) is crucial for insect reproduction, synthesized in the fat body and transported to oocytes by *Vg* receptor (*VgR*)-mediated endocytosis, a process known as vitellogenesis. *VgR*, belonging to the low-density lipoprotein receptor (LDLR) family (Sappington and Raikhel 1998, Tufail and Takeda 2009), is located on oocyte surfaces, ensuring *Vg* absorption for egg development (Tufail and Takeda 2005, Sheng et al. 2023). RNAi silencing of *Vg* or *VgR* in *Lasioderma serricorne* impairs ovarian development, shortens the oviposition period, decreases egg production, and lowers hatching rates (Guo et al. 2025). Inhibition of *FAMeT* and *JHAMT* expression downregulated *SfVg* transcription, which in turn resulted in a significant reduction in the reproductive capacity of female *Sogatella furcifera*.

Despite extensive characterization of *St1* in insect sugar transport, its direct mechanistic link to reproductive fitness remains unclear in hemipteran pests. In summary, we presume *St1* plays multiple roles in trehalose metabolism and reproduction. The gene encoding *St1* could potentially serve as a target for RNAi-based control strategies against insect pests in transgenic plants.

Materials and Methods

Insect Rearing

The rice variety used in the experiment was Taichung Native 1 (TN1). For this study, *N. lugens* were collected from field plots at the China National Rice Research Institute and reared in the laboratory for over 60 generations under controlled environmental conditions. The artificial climate chamber parameters were maintained as follows: temperature 27 ± 1 °C, relative humidity 65 ± 5%, photoperiod 18 L: 6 D (Light: Dark), indicating 18 h of light and 6 h of darkness per day.

dsRNA Synthesis and Microinjection

Total RNA was extracted from *N. lugens* using Trizol Reagent (Takara, Japan). RNA quality was assessed by 1% agarose gel electrophoresis, and concentration was determined with NanoDrop 2000 spectrophotometer (Thermo Fisher, United States). The extracted RNA was used as a template for cDNA transcription using the PrimeScript RT reagent Kit with gDNA Eraser (Takara, Japan). Specific primers were designed using Primer Premier 5.0 software for subsequent PCR amplification. Double-stranded RNA (dsRNA) was synthesized using the T7 RiboMAX Express RNAi System (Promega, United States). As a negative control, dsRNA targeting the green fluorescent protein (GFP) gene was synthesized under the same identical conditions. All primer sequences are listed in Table 1. Newly emerged long-winged female adults of *N. lugens* were microinjected with 100 nl of the synthesized dsRNA (4000 ng/μl) using the microinjection device TransferMan 4r microinjector (Eppendorf, Germany). Meanwhile, untreated males served as the control group.

Detection of Survival Rate and Reproduction of *N. lugens*

Fifty pairs of female *N. lugens* injected with ds*St1* and untreated males (1:1 ratio) were used and maintained on fresh TN1 rice seedlings. Meanwhile, the control group consisted of fifty pairs of ds*GFP*-injected female *N. lugens* and untreated males (1:1 ratio). Survival rates were monitored at 24 h intervals for 5 d, and statistical analysis was performed using the Log Rank Test (GraphPad Prism 9.0). Ovaries dissected from days 3 to 5 post-eclosion (80 in total) were histologically graded following the classification system of Lu et al. (2011), and mature oocytes were quantified under a stereomicroscope (Leica, Germany). On the third day of egg development in *N. lugens*, chitin begins to appear (Lu et al. 2022). Five females were randomly assigned to each group of clean rice seedlings and removed 3 d after oviposition. Daily recording of emerged nymphs continued

Table 1. Primers for dsRNA synthesis

Gene ID	Primer F (5'-3')	Primer R (5'-3')
111049718	CCTCGCTATGG-GTCCAAGTC	CCGCCAA-CATCCTGAAAGA
St1	ACCAGCGAAATA-AGTGAGAACG	GATTGATGCG-GAGATTAGAAGC
St11	CTCAGTTCCT-GGCAGCATT	GACTCGGG-CATCCATACAA
T7-primer	GGATCCTAATACGACTCACTATAGG	

Table 2. Primers for qRT-PCR

Gene ID	Primer F (5'-3')	Primer R (5'-3')
QSt1	CGGTTCCGATTGTCAGTTTG	TGCTGGTCCCTTGATCTGTG
QSt11	ATGTCTGATTGTCTTGGGAGGC	CCAAGTGAGAATACCACGATGAAC
QVg	CACTGCCCGTGCTGTGCTCTA	TGACTTCCTTGCTTTGCTCCC
QVgR	AGGCAGCCACACAGATAACCGC	AGCCGCTCGCTCCAGAACATT
QTRE1-1	GCCATTGTGGACAGGGTG	CGGTATGAACGAATAGAGCC
QTRE1-2	GATCGCACGGATGTTTA	AATGGCGTTCAAGTCAA
QTRE2	TCACGGTTGTCCAAGTCT	TGTTTCGTTTCGGCTGT
QTPS	AAGACTGAGGCGAATGGT	AAGGTGGAAATGGAATGTG
111049718	GTCGCCTTCTCCGCTATTCT	CCATGCCGTTTCCTCTTTG
Actin	TGGACTTCGAGCAGGAAATGG	ACGTCGCACTTCATGATCGAG

until 3 consecutive days with no eclosion. Residual unhatched eggs were enumerated through stem dissection. The preoviposition period and daily egg deposition were recorded from the beginning of the experiment until day 5, at 24 h intervals.

qRT-PCR

Five dsRNA-injected *N. lugens* specimens from each treatment group were selected for RNA extraction and cDNA synthesis, with each treatment group containing 3 biological replicates. qPCR primer sequences are listed in Table 2. The synthesized cDNA, diluted 5-fold, was used as templates for qRT-PCR analysis, with the *Actin* gene serving as an endogenous control. The qRT-PCR reaction mixture contained the following components: 3.2 µl ddH_2O, 5 µl TB Green Premix Ex Taq, 0.4 µl forward primer, 0.4 µl reverse primer, and 1 µl cDNA. Amplifications were performed using the Bio-Rad CFX96 Real-Time PCR Detection System (Bio-Rad, United States). Reaction specificity was verified through analysis of amplification and melting curves. Gene expression levels were quantified using the $2^{-\Delta\Delta CT}$ method (Livak and Schmittgen 2001). Data normalization was performed by calculating ΔCt as follows: ΔCt = Target gene Ct—Housekeeping gene Ct (*Actin*). ΔΔCt = ΔCt (treatment group)- ΔCt (mean of negative control group). The fold change in gene expression relative to the control group was then calculated as $2^{-\Delta\Delta CT}$.

Determination of Total Glycogen, Trehalose, Glucose Content and Trehalase Activity

Three days after dsRNA injection, 6 female *N. lugens* specimens were homogenized in PBS (1×, pH = 7.0) and lysed using the Bioruptor UCD-200 sonication system (Diagenode, Belgium) for 30 min. The homogenate was centrifuged at 1000 × *g* for 20 min at 4 °C and a 350 µl aliquot of the supernatant was used for quantification of total protein, glycogen and trehalose. The remaining supernatant was centrifuged again at 20,800 × *g* for 60 min at 4 °C. The resulting supernatant was used for glucose quantification, protein determination and soluble trehalase (TRE1) activity assays. In contrast, the pellet was resuspended in PBS (1×) for membrane-bound trehalase (TRE2) activity analysis and protein measurement. Protein concentrations were determined using a BCA Protein Assay Kit (Beyotime, China), glucose levels were measured using a Glucose Assay Kit (Sigma-Aldrich, United States) and trehalose quantification was performed using the Anthrone procedure. Absorbance was measured at 630 nm using a spectrophotometer. Protein concentrations were determined as previously described. Final trehalose content was expressed as the ratio of trehalose to protein concentration. The sensitivity of the method was evaluated based on the slope of the standard curve, since the slope is directly proportional to the method's ability to detect changes in trehalose. Through specific calculation procedures, the sensitivity of this method was determined to be 2.1039.

Data Analysis

Statistical analyses were performed using GraphPad Prism 9.0.0. In addition, Student's *t*-test was used to analyze the difference of data. Survival curves were analyzed with the Log Rank Test using GraphPad Prism 9.0.0. Significance thresholds were defined as follows: $^{*}P < 0.05$, $^{**}P < 0.01$, with non-significant difference ($P > 0.05$) marked as "ns." All data are expressed as mean ± SE.

Results

Effect of RNAi Interference on *St1*

Based on GO functional annotation and gene prediction, we identified 3 differentially expressed sugar transporter genes (*111052473*/*St1*, *111053675*/*St11*, and *111049718*) using data from ds*TREs* and validamycin treatments. qRT-PCR results demonstrated significant downregulation of *111049718* ($t = 11.25$; $df = 6$; $P < 0.0001$), *St1* ($t = 8.445$; $df = 6$; $P < 0.01$), and *St11* ($t = 14.95$; $df = 6$; $P < 0.0001$) following dsRNA injection, indicating effective RNAi-mediated suppression (Fig. 1a-c). Ovarian developmental patterns were comparable between the ds*St1*-treated and control groups ($t = 0.000$; $df = 4$; $P > 0.9999$) (Fig. 1d). Nevertheless, further investigation into potential subtle effects on reproductive inhibition is still necessary. Overall, the results indicated that while morphological characteristics remained unaltered, functional aspects such as fecundity were significantly affected. Additionally, *St1* was selected as a priority candidate for functional characterization due to its consistent transcript reduction.

Effects of ds*St1* on Survival and Reproduction of Female *N. lugens*

N. lugens females injected with ds*St1* exhibited significantly reduced survival rates ($\chi^2 = 6.019$; $df = 1$; $P = 0.0142$) compared to those injected with ds*GFP* during the 5-d post-injection period (Fig. 2a), indicating potential lifespan shortening effects of *St1* suppression. Although the preoviposition period in the ds*St1*-injected group showed a tendency to lengthen compared

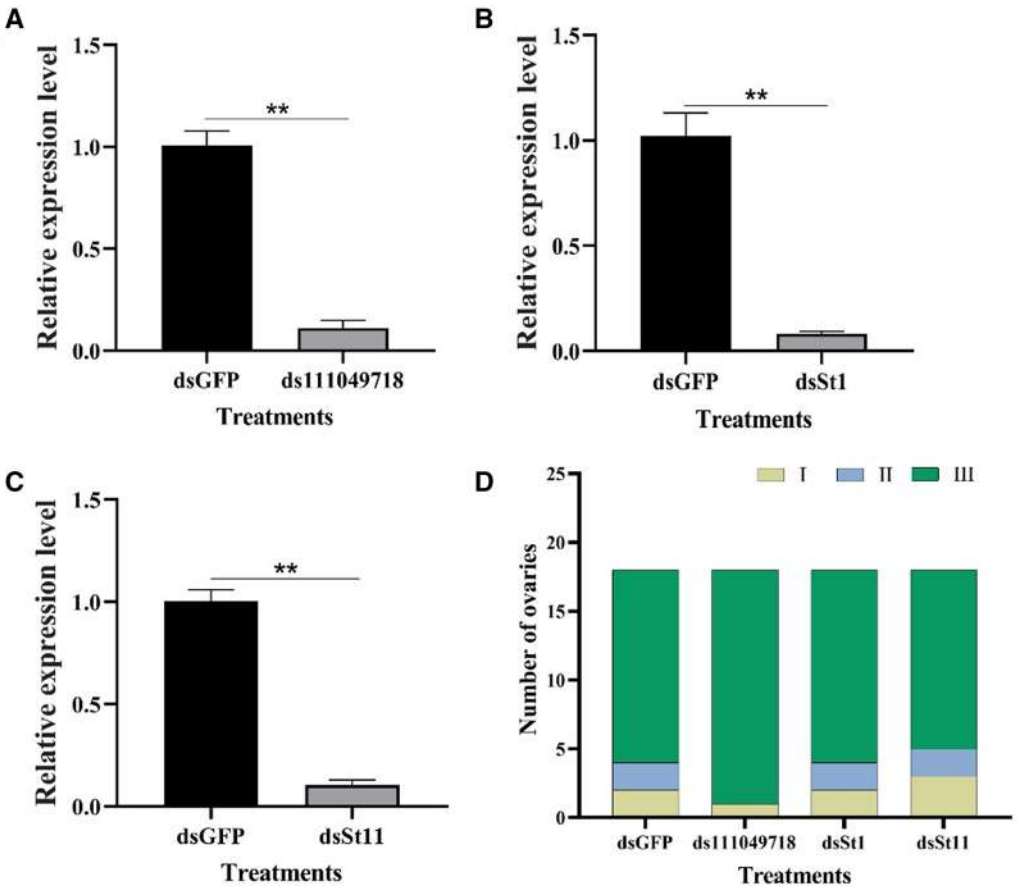

Fig. 1. RNAi effect of dsRNA on target genes 111049718 a), St1 b) and St11 c), and subsequent impacts of 3 sugar transporters on ovarian development d). The interference efficacy of dsRNA injection on genes 111049718, St1 and St11 was quantified (n = 3). Ovarian development in *N. lugens* was evaluated 3 d post-injection with ds111049718, dsSt1, and dsSt11 (n = 18). Grade I: Transparent stage, Grade II: Vitellogenesis stage, and Grade III: Matured stage. Data represent mean ± SE, analyzed using Student's *t* test (** $P < 0.01$, ns $P > 0.05$).

to the ds*GFP*-injected group, but there was no significant difference in the preoviposition period ($t = 1.524$; $df = 27$; $P = 0.1391$) between the 2 groups (Fig. 2b). However, compared with the ds*GFP*-injected group, the number of eggs laid in the ds*St1*-injected group decreased significantly ($t = 6.427$; $df = 27$; $P < 0.0001$) (Fig. 2c). In addition, there was no significant difference in the offspring hatching rate ($t = 2.274$; $df = 5$; $P = 0.0720$) between the ds*GFP* group and the ds*St1* group (Fig. 2d). These collective findings demonstrate that *St1* silencing has significant negative effects on adult longevity and reproductive output, while maintaining embryonic viability.

The Relative Expression of *Vg* and *VgR*

The results of qRT-PCR showed that the mRNA level of *Vg* was significantly lower than those in the control group on the third day in the ds*St1* treatment group ($t = 3.943$; $df = 6$; $P < 0.01$), and the mRNA level of *VgR* was also significantly lower ($t = 3.080$; $df = 5$; $P < 0.05$). These results indicate that ds*St1* inhibited the synthesis and transport of *Vg* (Fig. 3).

Changes of Sugar Content and Trehalase Activities after ds*St1* Injection

Following ds*St1* injection, the total glycogen content ($t = 4.635$; $df = 4$; $P < 0.01$) and glucose content ($t = 2.618$; $df = 6$; $P < 0.05$) in *N. lugens* decreased significantly, whereas trehalose levels remained unchanged ($t = 0.7628$; $df = 6$; $P = 0.4745$) (Fig. 4). These findings suggest that *St1* silencing specifically disrupts glycogen storage and glucose homeostasis without altering systemic trehalose pools. Soluble trehalase (TRE1) activity showed no significant variation ($t = 1.215$; $df = 14$; $P = 0.2443$), whereas membrane-bound trehalase (TRE2) activity was markedly reduced in ds*St1*-treated specimens ($t = 3.650$; $df = 5$; $P < 0.05$) (Fig. 5).

Expression of Trehalose Metabolism Genes after ds*St1* Injection

The synthesis of trehalose in *N. lugens* depends on trehalose-6-phosphate synthase (TPS), with 3 *TPS*-encoding genes (*TPS1*, *TPS2* and *TPS3*) having been identified in *N. lugens* (Yang et al. 2017). qRT-PCR analysis revealed that RNAi silencing of *St1* did not significantly affect the expression levels of *TPS1* ($t = 0.6302$; $df = 6$; $P = 0.5518$) (Fig. 6a) and *TPS2* ($t = 0.05924$; $df = 6$; $P = 0.9547$) (Fig. 6b). Although *TPS3* expression showed a marked decrease, this reduction did not reach statistical significance ($t = 1.121$; $df = 6$; $P = 0.3050$) (Fig. 6c). Furthermore, ds*St1* injection exhibited no significant impact on the expression of soluble trehalase genes *TRE1-1* ($t = 1.542$; $df = 6$; $P = 0.1741$) (Fig. 6d) and *TRE1-2* ($t = 0.4069$; $df = 5$; $P = 0.7009$) (Fig. 6e), but significantly suppressed the mRNA level of the membrane-bound trehalase gene *TRE2* ($t = 3.841$; $df = 5$; $P < 0.05$) (Fig. 6f).

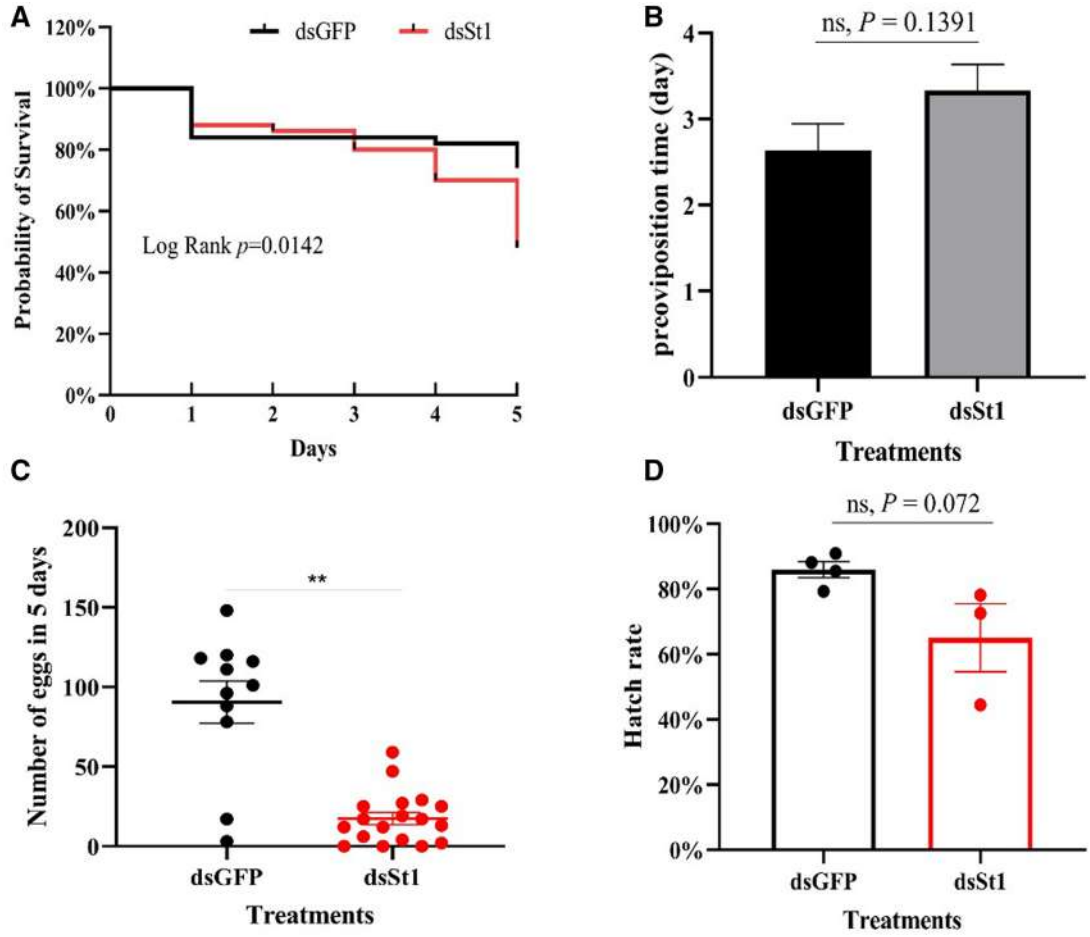

Fig. 2. Survival curve, preoviposition period, 5-d fecundity, and hatching rate of *N. lugens* following dsSt1 injection. a) Survival probability post-injection (n = 50), analyzed by Log Rank Test. b) Preoviposition period in females (2.636 ± 0.310 vs. 3.333 ± 0.302, n = 11). c) Total eggs laid within 5 d post-injection (n = 11). d) Offspring hatching rate with biological replicates (85.9175 ± 2.474 vs. 65.013 ± 10.413, n = 3). Data represent mean ± SE, statistical significance determined by Student's *t*-test (***P* < 0.01, ns *P* > 0.05).

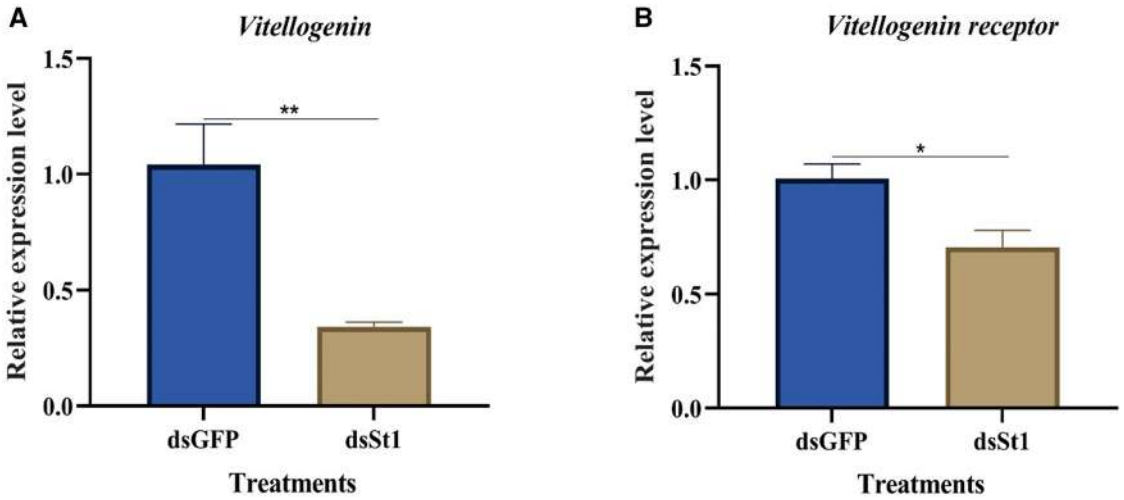

Fig. 3. Vitellogenin (A) and Vitellogenin receptor (B) expression profiles following dsSt1 intervention. Relative mRNA levels of Vitellogenin and Vitellogenin receptor were quantified 3 days post-injection via qRT-PCR using actin as the endogenous control (n = 3). Data represent mean ± SE, analyzed by Student's *t*-test (**P* < 0.05, ***P* < 0.01).

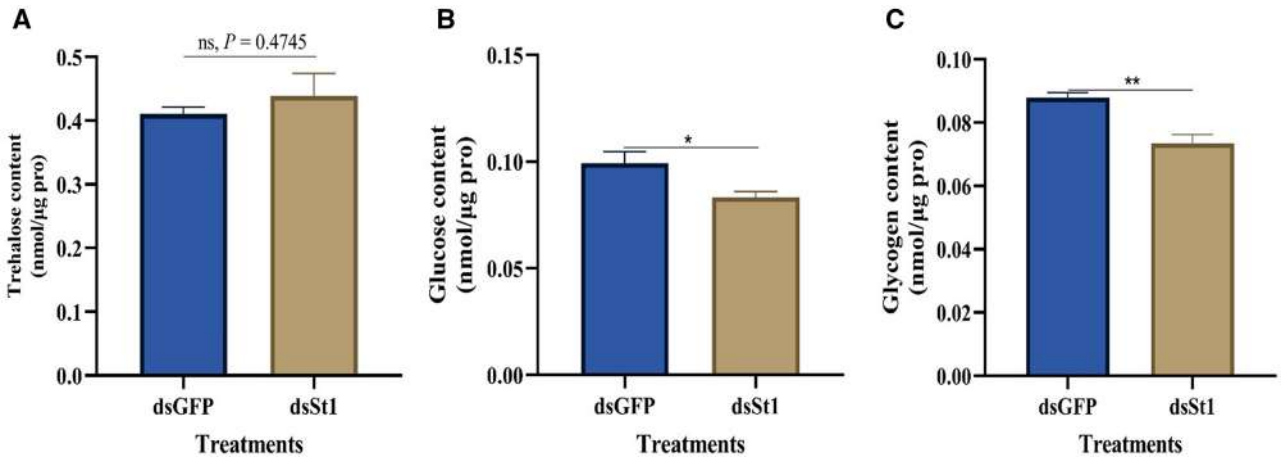

Fig. 4. Glycogen a), glucose b), and trehalose dynamics c) following dsSt1 injection. Metabolite concentrations in females were quantified 3 d post-injection (n = 3). Data represent mean ± SE, statistical significance determined by Student's *t*-test (ns $P > 0.05$, $*P < 0.05$, $**P < 0.01$).

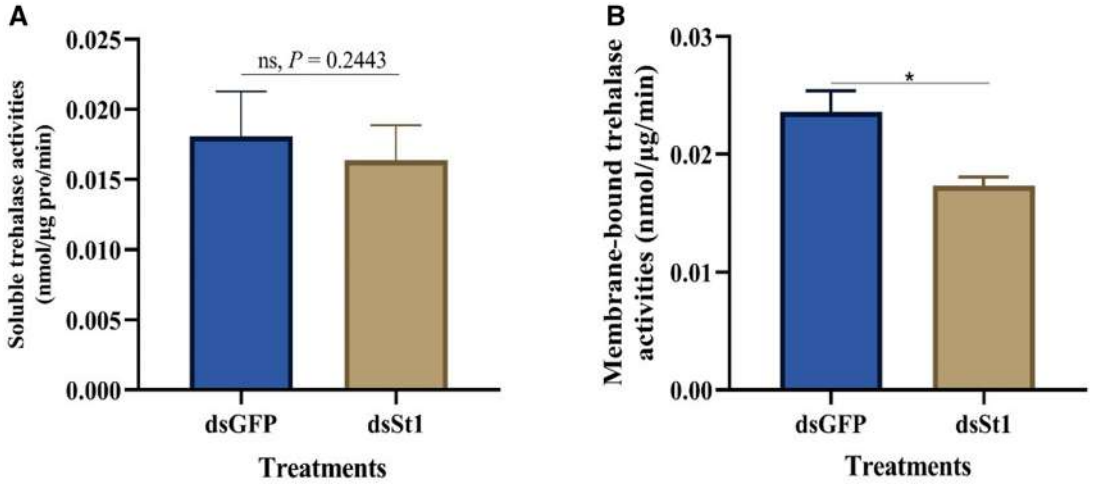

Fig. 5. Trehalase activity profiles following dsSt1 injection a-b). a) Soluble and b) membrane-bound trehalase activities were quantified in female adults 3 d post-injection (n = 3). Data represent mean ± SE, statistical significance determined by Student's *t*-test ($*P < 0.05$, ns $P > 0.05$).

Discussion

The data reported in this study strongly support our hypothesis that *St1* silencing lethally reduces *N. lugens* fitness in agroecosystems, as summarized below. Firstly, injection of ds*St1* reduced expression of *St1* transcript. Secondly, injection of ds*St1* resulted in a decreased female survival rate, diminished fecundity, diminished expression of both v*itellogenin* and its receptor gene, lowered glycogen and glucose contents, decreased trehalase activity, and reduced expression of genes involved in trehalose metabolism. Collectively, the uniformly deleterious changes observed in these biological performance parameters provide a compelling argument that *St1* can serve as a target for RNAi-based pest control strategies. *N. lugens* have 18 sugar transporter genes, but the mechanism of action of other sugar transporters remains to be explored.

Sugar transporter plays an important role in the growth and development of insects. *HaST24* (*Helicoverpa armigera* TRET-like sugar transporter 24) and *HaST36* are predominantly expressed during pupal stages, suggesting roles in diapause regulation and metamorphosis (Tellis et al. 2023). Furthermore, energy-intensive tissues, such as testes, ovaries, and flight muscles, require active sugar transport (Tang et al. 2018). Survival analysis revealed that ds*St1*-injected *N. lugens* exhibited significantly lower survival rates than the ds*GFP* control group (Fig. 2a), similar to the reduced survival reported by Ge et al. (2015). Consistent with these findings, the injection of ds*ST* (*SWEET1*) led to a significant reduction in *Spodoptera frugiperda* adult survival rates (Wan et al. 2021).

The research data significantly impacted the reproductive capacity of insects upon knockdown of the sugar transporter gene. Both ds*St1* injection (Fig. 2c) and ds*St6* treatment (Ge et al. 2015) significantly reduced egg-laying capacity, thus collectively demonstrating the critical role of sugar transporters in insect fecundity. qRT-PCR analysis further demonstrated that ds*St1* injection markedly decreased mRNA levels of *Vg* and *VgR*, indicating impaired synthesis and transport of vitellogenin (Fig. 3). Furthermore, studies have consistently shown across species that disruption of sugar transport pathways directly affects fecundity and embryonic development (Ye et al. 2021, Gu et al. 2023). The knockdown of *HaGlut4* in *Harmonia axyridis* significantly downregulates *Vg* and *VgR* expression, consequently it impairs ovarian development, disrupts oocyte maturation, and ultimately leads to a decrease in fecundity (Li et al. 2022). The knockdown of the *papilin*

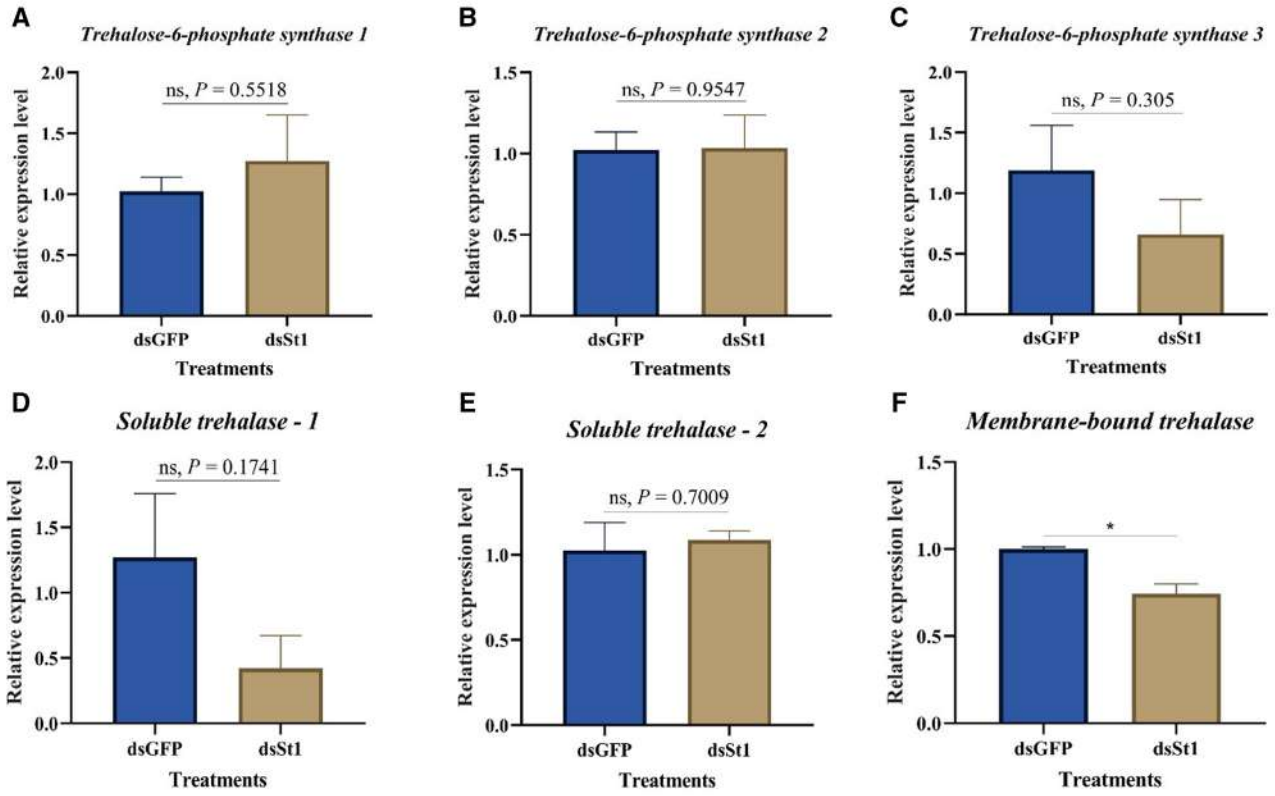

Fig. 6. Expression profiles of trehalose metabolism genes following dsSt1 injection a-f). a) Trehalose-6-phosphate synthase 1 (TPS1), b) TPS2, c) TPS3, d) soluble trehalase (TRE1)-1, e) TRE1-2, and f) membrane-bound trehalase (TRE2) mRNA levels were quantified 3 d post-injection via qRT-PCR (actin as endogenous control). Data represent mean ± SE (n = 3), statistical significance determined by Student's *t*-test (*$P < 0.05$, ns $P > 0.05$).

homologous gene (*NlPpn*) has been shown to severely impair egg hatching viability, suggesting that its function is related to development (Zhang et al. 2024).

Most insects typically maintain low glucose concentrations in their hemolymph. In contrast, trehalose, a disaccharide with higher molecular weight and slower diffusion rate than glucose, persists at high concentrations in hemolymph prior to cellular uptake (Yu et al. 2008, Leyria et al. 2021). The level of trehalose is related to insects' resistance to various environmental stresses (Benoit et al. 2009, Cornette et al. 2010), a conserved regulatory pattern demonstrated in *Drosophila melanogaster* studies, where optimization of glucose homeostasis ensures developmental stability (Xiong et al. 2016, Matsushita and Nishimura 2020). Treatment with ds*St1* inhibited the activity of *TRE* (Fig. 5), which was expected to lead to the accumulation of trehalose. However, the experimental results demonstrate that upon the cell's perception of this disturbance, a precise feedback and compensation mechanism is activated. On the one hand, the expression of *TRE* was down—regulated to further reduce the consumption of trehalose (Fig. 6d and f), and on the other hand, the expression of trehalose synthase genes was up—regulated to increase the supply of trehalose (Fig. 6a and b). This opposite regulatory effect on the 2 pathways of synthesis and degradation counteracts each other and finally effectively maintains the dynamic balance of intracellular trehalose levels (Fig. 4a). In *Helicoverpa armigera*, *HaSTs* expression is dynamically regulated in response to trehalose metabolism inhibition and abiotic stress, suggesting functional integration with metabolic adaptation and stress response. Specifically, silencing of *HaST69* impairs systemic trehalose accumulation, confirming its metabolic regulatory function (Liu et al. 2013, Tellis et al. 2023). Consistent with these observations, *Tret1-like* knockout in *Plutella xylostella* elevated whole-body trehalose levels, altered trehalase activity patterns, and redistributed trehalose between hemolymph and fat body compartments. These evidences suggested that *St1* inhibition disrupts glucose spatial distribution across tissues or cells through transport dysregulation, thereby perturbing broader carbohydrate metabolic networks in *N. lugens*. Knockout of *St1* specifically affects membrane-bound trehalase (*TRE2*) because they form a functionally tightly coupled unit on the cell membrane. The deletion of *St1* directly blocked the downstream of this unit, resulting in the accumulation of *TRE2* products and reverse regulation of its activity, but had no direct effect on soluble trehalase that was spatially and functionally independent. This phenomenon also highlights that the *TRE2*-sugar transporter system serves as a key pathway enabling *N. lugens* to efficiently obtain energy from the hemolymph. While our data demonstrate systemic metabolic alterations, the limitation is that the study did not assess subcellular nutrient distribution. Spatial omics approaches would be necessary to resolve compartment-specific effects.

Author Contributions

Yong-Kang Liu (Formal analysis [equal], Methodology [equal], Writing—original draft [equal], Writing—review & editing [equal]), Yanlin Luo (Formal analysis [equal], Methodology

[equal], Writing—original draft [equal], Writing—review & editing [equal]), Liwen Guan (Formal analysis [equal], Investigation [equal], Writing—review & editing [equal]), Sijing Wan (Supervision [equal], Writing—review & editing [equal]), Xianzhong Wang (Investigation [equal], Methodology [equal], Writing—review & editing [equal]), Caidi Xu (Validation [equal], Writing—review & editing [equal]), Binghua Xie (Writing—review & editing [equal]), Shigui Wang (Conceptualization [equal], Supervision [equal], Writing—review & editing [equal]), and Bin Tang (Conceptualization [equal], Funding acquisition [equal], Supervision [equal], Writing—review & editing [equal])

Supplementary Material

Supplementary material is available at *Journal of Economic Entomology* online.

Funding

This study was supported by the National Natural Science Foundation of China (Grant No. 32272608 and 32172415), the National Key Research and Development Program of China (Grant No. 2023YFE0104800), and by the ADOPT-IPM project funded by the European Union's Horizon Europe framework program (grant agreement number 101060430).

Conflicts of Interest

None declared.

Data Availability

Data in this study are available from the corresponding author.

References

Avonce N, Mendoza-Vargas A, Morett E, et al. 2006. Insights on the evolution of trehalose biosynthesis. *BMC Evol. Biol.* 6:109. https://doi.org/10.1186/1471-2148-6-109

Benoit JB, Lopez-Martinez G, Elnitsky MA, et al. 2009. Dehydration-induced cross tolerance of *Belgica Antarctica* larvae to cold and heat is facilitated by trehalose accumulation. *Comp. Biochem. Physiol. A Mol. Integr. Physiol.* 152:518–523. https://doi.org/10.1016/j.cbpa.2008.12.009

Chen LQ, Cheung LS, Feng L, et al. 2015. Transport of sugars. *Annu. Rev. Biochem.* 84:865–894. https://doi.org/10.1146/annurev-biochem-060614-033904

Cornette R, Kanamori Y, Watanabe M, et al. 2010. Identification of anhydrobiosis-related genes from an expressed sequence tag database in the cryptobiotic midge *Polypedilum vanderplanki* (Diptera; Chironomidae). *J. Biol. Chem.* 285:35889–35899. https://doi.org/10.1074/jbc.M110.150623

Ge LQ, Jiang YP, Xia T, et al. 2015. Silencing a sugar transporter gene reduces growth and fecundity in the brown planthopper, *Nilaparvata lugens* (Stål) (Hemiptera: Delphacidae). *Sci. Rep.* 5:12194. https://doi.org/10.1038/srep12194

Gokulanathan A, Mo HH, Park Y. 2024. Glucose influence cold tolerance in the fall armyworm, *Spodoptera frugiperda* via trehalase gene expression. *Sci. Rep.* 14:27334. https://doi.org/10.1038/s41598-024-79082-y

Gu SH, Lin PL, Chang CH. 2023. Expressions of sugar transporter genes during *Bombyx mori* embryonic development. *J. Exp. Zool. A Ecol. Integr. Physiol.* 339:788–798. https://doi.org/10.1002/jez.2729

Guo Q, Zu M, Liu D, et al. 2025. Roles of *Vitellogenin* and its receptor genes in female reproduction of the cigarette beetle, *Lasioderma sericorne*. *Insects* 16:175. https://doi.org/10.3390/insects16020175

Kikuta S, Kikawada T, Hagiwara-Komoda Y, et al. 2010. Sugar transporter genes of the brown planthopper, *Nilaparvata lugens*: a facilitated glucose/fructose transporter. *Insect Biochem. Mol. Biol.* 40:805–813. https://doi.org/10.1016/j.ibmb.2010.07.008

Leyria J, El-Mawed H, Orchard I, et al. 2021. Regulation of a trehalose-specific facilitated transporter (*TRET*) by insulin and adipokinetic hormone in *Rhodnius prolixus*, a vector of chagas disease. *Front. Physiol.* 12:624165. https://doi.org/10.3389/fphys.2021.624165

Li Y, Wang SS, Wang S, et al. 2022. Involvement of glucose transporter 4 in ovarian development and reproductive maturation of *Harmonia axyridis* (Coleoptera: Coccinellidae). *Insect Sci.* 29:691–703. https://doi.org/10.1111/1744-7917.12972

Liu K, Dong Y, Huang Y, et al. 2013. Impact of trehalose transporter knockdown on *Anopheles gambiae* stress adaptation and susceptibility to *Plasmodium falciparum* infection. *Proc. Natl. Acad. Sci. USA* 110:17504–17509. https://doi.org/10.1073/pnas.1316709110

Livak KJ, Schmittgen TD. 2001. Analysis of relative gene expression data using real-time quantitative PCR and the $2^{-\Delta\Delta CT}$ method. *Methods* 25:402–408. https://doi.org/10.1006/meth.2001.1262

Lu F, Qi GJ, Qin RR, et al. 2011. The processes of morphological change and grading criteria for ovarian development in the brown planthopper. *Chin. J. Appl. Entomol.* 48:1394–1400. https://doi.org/10.7679/j.issn.2095-1353.2011.218.

Lu JB, Guo JS, Chen X, et al. 2022. Chitin synthase 1 and five cuticle protein genes are involved in serosal cuticle formation during early embryogenesis to enhance eggshells in *Nilaparvata lugens*. *Insect Sci.* 29:363–378. https://doi.org/10.1111/1744-7917.12937

Matsushita R, Nishimura T. 2020. Trehalose metabolism confers developmental robustness and stability in *Drosophila* by regulating glucose homeostasis. *Commun. Biol.* 3:170. https://doi.org/10.1038/s42003-020-0889-1

Price DR, Wilkinson HS, Gatehouse JA. 2007. Functional expression and characterisation of a gut facilitative glucose transporter, *NlHT1*, from the phloem-feeding insect *Nilaparvata lugens* (rice brown planthopper). *Insect Biochem. Mol. Biol.* 37:1138–1148. https://doi.org/10.1016/j.ibmb.2007.07.001

Qin Y, Xu P, Jin R, et al. 2021. Resistance of *Nilaparvata lugens* (Hemiptera: Delphacidae) to triflumezopyrim: inheritance and fitness costs. *Pest Manag. Sci.* 77:5566–5575. https://doi.org/10.1002/ps.6598

Sappington TW, Raikhel AS. 1998. Ligand-binding domains in vitellogenin receptors and other LDL-receptor family members share a common ancestral ordering of cysteine-rich repeats. *J. Mol. Evol.* 46:476–487. https://doi.org/10.1007/pl00006328

Sheng Y, Chen J, Jiang H, et al. 2023. The vitellogenin receptor gene contributes to mating and host-searching behaviors in parasitoid wasps. *iScience* 26:106298. https://doi.org/10.1016/j.isci.2023.106298

Shukla E, Thorat LJ, Nath BB, et al. 2015. Insect trehalase: physiological significance and potential applications. *Glycobiology* 25:357–367. https://doi.org/10.1093/glycob/cwu125

Tang B, Wang S, Wang SG, et al. 2018. Invertebrate trehalose-6-phosphate synthase gene: genetic architecture, biochemistry, physiological function, and potential applications. *Front. Physiol.* 9:30. https://doi.org/10.3389/fphys.2018.00030

Tang B, Xu K, Liu Y, et al. 2022. A review of physiological resistance to insecticide stress in *Nilaparvata lugens*. *3 Biotech* 12:84. https://doi.org/10.1007/s13205-022-03137-y

Tang B, Yang M, Shen Q, et al. 2017. Suppressing the activity of trehalase with validamycin disrupts the trehalose and chitin biosynthesis pathways in the rice brown planthopper, *Nilaparvata lugens*. *Pestic. Biochem. Physiol.* 137:81–90. https://doi.org/10.1016/j.pestbp.2016.10.003

Tellis MB, Chaudhari BY, Deshpande SV, et al. 2023. Trehalose transporter-like gene diversity and dynamics enhances stress response and recovery in *Helicoverpa armigera*. *Gene* 862:147259. https://doi.org/10.1016/j.gene.2023.147259

Tufail M, Takeda M. 2005. Molecular cloning, characterization and regulation of the cockroach vitellogenin receptor during oogenesis. *Insect Mol. Biol.* 14:389–401. https://doi.org/10.1111/j.1365-2583.2005.00570.x

Tufail M, Takeda M. 2009. Insect vitellogenin/lipophorin receptors: molecular structures, role in oogenesis, and regulatory mechanisms. *J. Insect Physiol.* 55:87–103. https://doi.org/10.1016/j.jinsphys.2008.11.007

Wan XS, Shi MR, Xu J, et al. 2021. Interference Efficiency and Effects of Bacterium-mediated RNAi in the Fall Armyworm (Lepidoptera: Noctuidae). *J. Insect Sci.* 21:8. https://doi.org/10.1093/jisesa/ieab073

Wang LX, Tao S, Zhang YC, et al. 2022. Overexpression of ATP-binding cassette transporter Mdr49-like confers resistance to imidacloprid in the field populations of brown planthopper, *Nilaparvata lugens*. *Pest Manag. Sci.* 78:579–590. https://doi.org/10.1002/ps.6666

Xiong KC, Wang J, Li JH, et al. 2016. RNA interference of a trehalose-6-phosphate synthase gene reveals its roles during larval-pupal metamorphosis in *Bactrocera minax* (Diptera: Tephritidae). *J. Insect Physiol.* 91–92:84–92. https://doi.org/10.1016/j.jinsphys.2016.07.003

Yang B, Lin X, Yu N, et al. 2020. Contribution of glutathione s-transferases to imidacloprid resistance in *Nilaparvata lugens*. *J. Agric. Food Chem.* 68:15403–15408. https://doi.org/10.1021/acs.jafc.0c05763

Yang M, Zhao L, Shen Q, et al. 2017. Knockdown of two trehalose-6-phosphate synthases severely affects chitin metabolism gene expression in the brown planthopper *Nilaparvata lugens*. *Pest Manag. Sci.* 73:206–216. https://doi.org/10.1002/ps.4287

Ye Z, Liu F, Ferguson ST, et al. 2021. Ammonium transporter AcAmt mutagenesis uncovers reproductive and physiological defects without impacting olfactory responses to ammonia in the malaria vector mosquito *Anopheles coluzzii*. *Insect Biochem. Mol. Biol.* 134:103578. https://doi.org/10.1016/j.ibmb.2021.103578

Yu CH, Lu D, Lin RH, et al. 2008. Trehalose—the blood sugar in insects. *Chin. J. Appl. Entomol.* 5:832–837. https://doi.org/10.3969/j.issn.0452-8255.2008.05.035

Zhang C, Zhang JY, Wang N, et al. 2024. RNAi-mediated knockdown of papilin gene affects the egg hatching in *Nilaparvata lugens*. *Pest Manag. Sci.* 80:4779–4789. https://doi.org/10.1002/ps.8194

Zhao L, Yang M, Shen Q, et al. 2016. Functional characterization of three trehalase genes regulating the chitin metabolism pathway in rice brown planthopper using RNA interference. *Sci. Rep.* 6:27841. https://doi.org/10.1038/srep27841

Zheng X, Zhu L, He G. 2021. Genetic and molecular understanding of host rice resistance and *Nilaparvata lugens* adaptation. *Curr. Opin. Insect Sci.* 45:14–20. https://doi.org/10.1016/j.cois.2020.11.005

Zhou M, Shen Q, Wang S, et al. 2022. Regulatory function of the trehalose-6-phosphate synthase gene *TPS3* on chitin metabolism in brown planthopper, *Nilaparvata lugens*. *Insect Mol. Biol.* 31:241–250. https://doi.org/10.1111/imb.12754